DR ROGER D CONE (Orcid ID : 0000-0003-3333-5651)

Author Manuscript

Article type : Original Article

Late onset obesity in mice with targeted deletion of potassium inward rectifier Kir7.1 from cells expressing the melanocortin-4 receptor

E. J. P. Anderson[1], M. Ghamari-Langroudi[1], I. Cakir[1,2], M. J. Litt[1], Valerie Chen[3], Roman E. Reggiardo[3], Glenn L. Millhauser[3], R. D. Cone[1,2,4*]

[1]Department of Molecular Physiology and Biophysics, Vanderbilt University, Nashville, Tennessee

[2]Life Sciences Institute, University of Michigan, Ann Arbor, Michigan

[3]Department of Chemistry and Biochemistry, University of California Santa Cruz, Santa Cruz, California

[4]Department of Molecular and Integrative Pharmacology, School of Medicine, University of Michigan, Ann Arbor, Michigan

Short Title: Deletion of Kir7.1 from MC4R Cells in Mice

This is the author manuscript accepted for publication and has undergone full peer review but has not been through the copyediting, typesetting, pagination and proofreading process, which may lead to differences between this version and the Version of Record. Please cite this article as doi: 10.1111/jne.12670

This article is protected by copyright. All rights reserved

Key Words: Melanocortin-4 receptor, MC4R, Kir7.1, kcnj13, obesity

*Correspondence
Roger D. Cone
Life Sciences Institute
210 Washtenaw Ave.
Ann Arbor, MI 48109
E-mail: rcone@umich.edu

Author Manuscript

Abstract

Energy stores in fat tissue are determined in part by the activity of hypothalamic neurons expressing the melanocortin-4 receptor (MC4R). Even partial reduction in MC4R expression levels in mice, rats, or humans produces hyperphagia and morbid obesity. Thus, it is of great interest to understand the molecular basis of neuromodulation by the MC4R. The MC4R is a G protein-coupled receptor that signals efficiently through $G\alpha_S$, and this signaling pathway is essential for normal MC4R function *in vivo*. However, previous data from hypothalamic slice preparations indicated that activation of the MC4R depolarized neurons through G protein-independent regulation of the ion channel Kir7.1. We showed here that deletion of *Kcnj13*, the gene encoding Kir7.1, specifically from MC4R neurons produced resistance to melanocortin peptide-induced depolarization of MC4R PVN neurons in brain slices, resistance to the sustained anorexic effect of exogenously administered melanocortin peptides, late onset obesity, increased linear growth, and glucose intolerance. Some MC4R-mediated phenotypes appeared intact, including AgRP-induced stimulation of food intake, and MC4R-mediated induction of PYY release from intestinal L cells. Thus, a subset of the consequences of MC4R signaling *in vivo* appear dependent on expression of the Kir7.1 channel in MC4R cells.

This article is protected by copyright. All rights reserved

Author Manuscript

1 | INTRODUCTION

Haploinsufficiency of the MC4R in humans is the most common monogenic cause of severe obesity known, accounting for up to 5% of cases [1 2]. The composite prevalence of obesity-causing deleterious alleles in the human population has been demonstrated to be approximately 1/1500 [3], and a detailed clinical picture of the syndrome has been reported [4 5]. Remarkably, the syndrome is virtually identical to that reported for the mouse [6 7 8] with increased adipose mass, lean mass, linear growth, hyperinsulinemia, and severe hyperphagia. Genome-wide association studies have also identified SNPs adjacent to the *MC4R* gene that are associated with obesity [9 10 11]. These non-coding changes also support the notion that small changes in the expression level or activity of the MC4R may impact adiposity. Humans with haploinsufficiency, or even homozygous null status at the *MC4R* are relatively normal outside of the obesity syndrome, with only mild hypotension and hyperinsulinemia reported. Another unique feature of the central melanocortin system are the gene dosage effects for *MC4R* [12 8], a highly unusual finding for G protein-coupled receptor signaling systems.

The MC4R is thus a well-validated target for the treatment of common obesity (8, 9), and cachexia [13 14 15 16]. Other studies suggest potential applications in diabetes [7 17 18] and metabolic syndrome [19 20], depression-related anorexia and anhedonia [21], and obsessive-compulsive disorder [22]. The MC4R appears to be at the heart of the adipostat, in that administration of melanocortin agonists inhibits food intake [12] and increases energy expenditure [23]. Chronic administration of potent melanocortin agonists produces

This article is protected by copyright. All rights reserved

significant weight loss in model systems from rodents, to primates [24]. However, clinical trials of potent small molecule orthosteric agonists of the MC4R have failed due to target-mediated pressor effects. Despite the target-mediated pressor response resulting from most melanocortin agonists, two peptide analogues of the native MC4R ligand, α-MSH, have been demonstrated to cause weight loss without a pressor response [24,25,26,27]. One of these compounds, setmelanotide, has been used successfully in a clinical trial in two patients with compound heterozygous mutations in proopiomelanocortin (POMC), the preprohormone precursor for α-MSH [24], and in a clinical trial in patients with homozygous mutations in the gene encoding the leptin receptor [28]. There is no data available explaining why some MC4R agonists are capable of inducing weight loss without the target-mediated pressor response, although biased agonism must be considered in the event that multiple signaling pathways are activated downstream of MC4R.

In this regard, it is already appreciated that MC4R exhibits different signaling modalities on the cellular level *in vivo*. The MC4R couples to $G\alpha_S$ in all cells tested, and it has been demonstrated that deletion of $G\alpha_S$ from MC4R neurons recapitulates the phenotype seen in MC4R knockout mice [29]. However, the complexity of MC4R signaling *in vivo* is also clear. α-MSH activates MC4R positive IML neurons via a putative non-specific cation channel [30], but inhibits MC4R neurons in the DMX via activation of a K_{ATP} channel [31]. Recently, we demonstrated using a hypothalamic slice preparation in the mouse, that α-MSH appears to depolarize and activate MC4R neurons in the PVN via a G protein independent mechanism involving inhibition of the inward rectifier channel Kir7.1 [32]. This is a highly unusual finding, requiring further validation *in vivo*. Furthermore, a better understanding of the role(s) of variant MC4R signaling modalities *in vivo* might lead to a rationale pharmacological approach to the development of small molecule biased agonists of MC4R that could discriminate between weight loss and pressor activities. Towards these two goals, we specifically deleted the inward rectifier Kir7.1 from MC4R cells in the mouse, and conducted pharmacological and physiological studies of the resulting animals.

This article is protected by copyright. All rights reserved

Author Manuscript

2 | MATERIALS AND METHODS

2.1 | Mouse strains and genotyping

We used promoter-driven, knockout-first, *Kcnj13* targeted selection clones from the Knockout Mouse Project (KOMP) Repository at UCDavis for the generation of our transgenic mice. Embryonic stem cell (ESC) clones expressing the mutant allele *Kcnj13*$^{tm1a(KOMP)wtsi}$ were expanded at Vanderbilt's Transgenic Mouse / ES Cell Shared Resource (TMESCSR), where chimeric mice were generated on the C57BL/6N background. Germ line transmission was confirmed by crossing chimeric male mice to wildtype C57BL/6N females. Genotyping confirmed the presence of the mutant allele, *Kcnj13*$^{tm1a(KOMP)wtsi}$, in progeny. This allele also carries an En2 splice acceptor sequence and a poly-A transcription termination signal, which disrupts *Kcnj13* gene function. Following the KOMP breeding strategy for mutant allele generation, *Kcnj13*$^{tm1a(KOMP)wtsi}$ mice were bred to mice expressing the recombinase flippase to generate the *Kcnj13*$^{tm1c(KOMP)wtsi}$ allele. The expression of FLP recombinase excised the promoter driven Neo cassette, converting allele *tm1a* into conditional mutant allele *tm1c*. Mutant *Kcnj13*$^{tm1c(KOMP)wtsi}$ mice were mated to sibling mice in order to build a colony of *Kcnj13*^{tm1c} mice (referred to as *Kcnj13*$^{fl/fl}$ mice). The *Kcnj13*$^{fl/fl}$ colony was crossed with a MC4R-t2A-Cre Tg/+ line (kindly provided by Dr. Bradford Lowell) to generate a MC4R cell specific *Kcnj13* knockout experimental animal (referred to as *Kcnj13ΔMC4R*^{Cre}). This allele is referred to as *Kcnj13*^{tm1d} in KOMP nomenclature. All mouse lines were maintained on a C57BL/6NJ background with annual backcrosses to wild type C57BL/6NJ mice (Jackson Laboratory; Sacramento, California - Jax Stock No: 005304).

Mc4r-tau-Sapphire mice for electrophysiological studies were obtained from the Jackson Laboratory (Jax Stock No: 008323).

Primers for genotyping Kcnj13$^{fl/fl}$ or Kcnj13$^{+/+}$ alleles were:
*Kcnj13*_ttR CCAGAGGGTGAGGCTTATAATTTGTGC
*Kcnj13*_F GGTCAGTGAGATATGGCCTAGTGGG

This article is protected by copyright. All rights reserved

Author Manuscript

2.2 | Mouse handling

All mice were housed in standard, infection–free housing conditions at 25°C, in a facility on a 12 hr light:12 hr dark cycle. Strictly pathogen-free quality of the mouse colonies was maintained through quarterly serology, quarterly histopathologic exams, and daily veterinarian monitoring of the general health and welfare of animals. Male and female mice were used for these experimental procedures. Mice were weaned at four weeks of age and kept with 4-5 mice per cage, unless animals were used for feeding studies. Animals used in feeding analysis were singly housed for acute studies and dually housed for long term feeding studies. Unless otherwise described, all mice were fed a standard chow diet (Lab Diet; St. Louis, MO; S-5LOD - 13.5 kcal% fat, 32.98 kcal% protein, 56.7 kcal% carbohydrate). Diet induced obesity was promoted by high fat diet (Research Diets; New Brunswick, NJ; D12492 - 60 kcal% fat, 20 kcal% protein, 20 kcal% carbohydrate). Post mortem studies were conducted by giving animals a dose of 5mg/kg tribromoethanol in order to deeply anesthetize the mice before sacrifice via decapitation. Tissues of interest were rapidly excised and flash frozen by liquid nitrogen. All procedures were carried out with approval from the Institutional Animal Care and Use Committee of Vanderbilt University Medical Center.

2.3 | Hypothalamic slice electrophysiology

Mc4r-tau-Sapphire mice, backcrossed onto the C57BL/6J background, were previously characterized by dual immunohistochemistry and *in situ* hybridization to validate that GFP-positive neurons in the PVN expressed MC4R RNA [33]. Randomly selected MC4R-GFP male and female mice, 8–16 weeks of age, were deeply anaesthetized with isoflurane before decapitation. The brain was entirely removed and immediately submerged in ice-cold, gassed (95% O_2, 5% CO_2) artificial cerebrospinal fluid (aCSF), containing (in mM): 126.2 NaCl, 3.1 KCl, 2 $CaCl_2$, 1 $MgCl_2$, 1 NaH_2PO_4, 26.2 $NaHCO_3$, 10 glucose and 11 sucrose (320 mosm per kg, pH 7.39 when gassed with 95% O_2, 5% CO_2 at room temperature). Brain blocks containing

This article is protected by copyright. All rights reserved

Author Manuscript

hypothalamus were made by trimming whole brains while the brains were immersed in oxygenated, near-freezing aCSF and glued to a dental-cement cast customized to the size of the block mounted on a plate with adjustable angle. Brain slices of 200-μm thicknesses were then cut at angle range between 44° and 49° in reference to horizontal plane and transferred to a glass beaker containing oxygenated ACSF at 31 °C. After an incubation period lasting at least one hour, a slice was transferred to a recording chamber (about 2.0 ml in volume), then submerged and immobilized with nylon strands drawn taut across a C-shaped platinum wire (1 mm outer diameter), and perfused with warmed (31–32 °C) oxygenated ACSF at a rate of 2–3 ml min^{-1}. EGFP-fluorescent neurons were unambiguously identified and patched using combined epifluorescence and IR-DIC optics. Fluorescent neurons of healthy IR-DIC appearance but of every level of fluorescence brightness were chosen for electrophysiological recordings. Drugs were added to aCSF and bath applied to the slice via the perfusion system for extracellular applications. The small volume of the recording chamber relative to the flow rate assured a complete exchange of solution occurring in less than 1 min. The persisting effects of a peptide were therefore due to prolonged effects rather than a slow wash out.

In this study, whole-cell patch-clamp recordings were used to obtain information about action potential firing activity, and membrane potentials and currents. Unless stated otherwise, whole cell recordings were performed using patch pipettes of 3.4 MΩ to 5 MΩ resistance when filled with a solution containing (in mM); 125 K gluconate, 8 KCl, 4 $MgCl_2$, 10 HEPES, 5 NaOH, 4 Na_2ATP, 0.4 Na_3GTP, 5 Na_2-creatine phosphate, 7 sucrose and 7 KOH which resulted in a pH ~7.23 and osmolality of 295–300 mosmol per kg. The permeability of the α-MSH regulated channels was investigated by replacing K gluconate and KCl with 130 RbCl and 4 KCl, but otherwise similar condition. The examination of effects of Mg^{2+}-free internal solution on the α-MSH-induced current was conducted in voltage clamp mode from PVN neurons held at −55 mV. The Mg^{2+}-free internal solution contained 103 K-gluconate, 30 KCl, 10 HEPES-KOH, 0.5 $CaCl_2$, 5.5 EDTA-KOH, pH 7.23, with osmolality 304 mosmol per kg. The ATP free solution contained 83 K-gluconate, 30 KCl, 10 HEPES-KOH, 0.5 $CaCl_2$, 4 $MgCl_2$, 5.5 EGTA-KOH, pH 7.2 and osmolality

This article is protected by copyright. All rights reserved

Author Manuscript

298 mosmol per kg. Neuronal integrity was assessed by all of the following: small holding current (≤30 pA at −70 mV) when voltage-clamped, large amplitude rebound spikes, the ability to fire and lack of obvious morphological deterioration (that is, lack of blebbing and nucleus not visually present).

In order to quantify the action potential firing and amplitude of depolarization induced by α-MSH, current clamp recordings were performed in continuous mode while the membrane potential of neurons were held between −55 and −60 mV to prevent continuous spontaneous action potential firing. The firing frequency and membrane potential of neurons was measured during a 3-min period before the application of the peptides, and for another 3-min period 7–11 min after administration of peptide, and results compared.

Data were acquired at 10 kHz using a MultiClamp 700A amplifier (2,000× gain, –3 dB filter frequency 5 kHz) and Clampex 10.0.1 software (Axon Instruments, Union City, CA). GraphPad Prism 5.0 (Graphpad Software, Inc., San Diego, CA) and Excel 2010 (Microsoft) were used for data analysis. Statistical tests used included the paired *t*-test, when examining response of the same neurons before and after treatment with a compound, and the unpaired *t*-test when comparing the responses of different sets of neurons.

2.4 | Fast-induced refeeding

Age and litter matched male and female mice were used for this study from young (not shown) and mature, 35-45 weeks of age, cohorts. Studies were repeated at least three times across multiple cohorts. One week before the study, mice were singly housed and accustomed to handling with IP injections of 100µl saline while provided with *ab libitum* standard chow and water. One day before the study mice were moved to clean cages with fresh bedding to minimize coprophagia. Mice were food deprived for 16-24 hours, before drug was administered at the beginning of dark cycle.

Mice were food deprived for 16 h before drug treatment, starting shortly before the beginning of the dark cycle. Experiments were blinded; drug compounds were prepared and coded the morning of the injections by an individual who would not be

This article is protected by copyright. All rights reserved

Author Manuscript

conducting the experiment. The randomly selected experimental groups consisted of animals that were given vehicle, 10.0 mg/kg saline or 10.0 mg/kg of the melanocortin agonist LY2112688 (LY). For repeated studies, animals rested at least seven days between fasting periods and opposite treatments were given. Numbers needed to achieve significant inhibition of food intake by a melanocortin compound versus saline were based on prior experience. Food intake was measured at multiple time points after injection, beginning at 2 hours and extending as far as 40 hours after injection. In viral knockdown studies a ground feeding cylinder canister with a wire mesh bottom was used rather than the cage hopper. Mice were accustomed to the presence of the canister in their cage for one week before the experiment. The reduced accessibility of this apparatus is reflected in the reduced chow consumption in viral knockdown mice compared to cell specific genetic deletion mice studies. Statistical significance was established using two-way ANOVA and Tukey's post-hoc with a $P < 0.05$ significance value.

2.5 | shRNA lentiviral design and hypothalamic injection

Mouse *Kcnj13* shRNA and scramble shRNA were constructed using the vector pSico (Addgene). *Kcnj13* shRNA plasmid (TRCN0000262099; Fig. S3 clone #99) was from Sigma, St. Louis, MO with sequence: CCGGCGCCTTACTTGCCATACAAATCTCGAGATTTGTATGGCAAGTAAGGCGTTTTTG. Scramble shRNA (plasmid# 1864) was purchased from Addgene. Scramble shRNA construct in pLKO.1 vectors was subcloned into pLL3.7 (Addgene, plasmid #:11795), which also encodes GFP. pLL3.7 plasmid with shRNA (scramble vs. *Kcnj13*). *Kcnj13* shRNA sequence (Fig. S3) was cloned into pLKO.1 expressing mCherry.

293T cells were transfected with 12.6 µg of plasmids containing the shRNA (scramble vs. Kcnj13), and 6.3 µg each of the following plasmids: pRSV-Rev, pVSVG, and pMDLp/g (gift of Dr. Roger Colbran) using Lipofectamine 2000 (Invitrogen, Carlsbad, CA) on 15 cm dishes. 96 hours post-transfection, culture medium from five 15cm-plates per shRNA clone were collected, and filtered through a 0.45µm filter. Viral particles were isolated by ultracentrifugation at 4°C, 26000 rpm

This article is protected by copyright. All rights reserved

Author Manuscript

for 2 hours using a SW32Ti rotor. The pellet was resuspended in sterile PBS, aliquoted and frozen at -80 ˚C until further use.

Viral titer was quantified as follows: 100,000 293T cells were plated on 24-well plates. Cells were transduced by ten-fold serial dilutions of the viral particles with dilution range between 1:10 – $1:10^5$ using polybrene. GFP (for scramble shNA) or mCherry (for shRNA against *Kcnj*13) positive cells were counted in triplicate. Purified lentivirus suspended in 550-600 nl artificial CSF was injected bilaterally and infused over 15 minutes into the PVN using a stereotactic frame and the coordinates of 0.82 mm posterior to bregma, 0.31 mm lateral to the midline of the brain and 4.68 mm below the surface of the skull, via a 26-gauge guide cannula and a 33-gauge internal injector (Plastics One, Roanoke, VA) connected to a 2 µl Hamilton syringe.

2.6 | Cannulation surgery for intracerebroventricular injection

To study the effect of ICV injection of MC4R neuropeptide, mice were anesthetized with isoflurane and a stainless-steel cannula (Plastics One, Roanoke, VA) was surgically implanted into the right lateral ventricle using the stereotaxic coordinates of 0.46 mm posterior to the bregma, 1.0 mm lateral to the midline, and 2.2 mm below the surface of the skull. Mice were allowed to recover for approximately 5 days while monitoring food intake and body weight with acclimatization to handling and manipulation of the dummy cannula. After recovery, cannula placement was verified by injecting 10 ng angiotensin II (Sigma) diluted in 0.5 µl sterile saline. Animals that did not exhibit drinking response within 30 minutes were excluded from the study. A day later experimental procedures were initiated during the light cycle. Peptides ($AgRP_{83-132}$, kindly provided by Glenn Millhauser) or vehicle were infused in a 0.5 µl volume over a 1-min period with a 2.0 µl Hamilton syringe (Plastics One) coupled to an injection cannula by a polyethylene tubing. After injection the injector was kept in place for 1-min to ensure diffusion from the injector tip. Food intake and body weight was monitored after injection. When experimental procedures concluded, cannula placement was also verified histologically.

2.7 | Plasma hormone measurements

This article is protected by copyright. All rights reserved

Author Manuscript

Male and female experimental mice (*Kcnj13ΔMC4R*^{Cre}; *Kcnj13*$^{fl/fl}$) age 25-27 weeks were acclimated to scruffing and injections for up to 5 days prior to blood collection. The day of the study, postprandial plasma PYY was reduced to baseline levels by a 6 h daytime fast. Mice were randomly selected to receive intraperitoneal injection of vehicle (saline) or 5 mg/kg of LY2112688 in 100-200 uL volumes according to body weight. Numbers chosen based on prior experience suggesting significance can be achieved with 6 animals per treatment. At 10 min post-injection, approximately 200 µl of blood was collected via submandibular bleeding in conscious mice or by decapitation under anesthesia for trunk bleed. Blood was collected into vials containing appropriate volumes of EDTA and protease inhibitor cocktail for mammalian tissues (Sigma P8340) to prevent degradation of PYY and kept on ice. Upon collection of all blood samples, the vials were spun at 3000 X G at 4°C for 30 minutes. Plasma was removed and spun at 10000 × G at 4°C for 1 minute to pellet remaining blood cells. Plasma was frozen at −80°C until PYY was assayed. Plasma hormones were assayed in 10 µL duplicate samples using the MilliplexMAP Mouse Metabolic Hormone - Magnetic Bead Panel Immunoassay (Millipore MMHMAG-44K 1-plex kit for total PYY), with undiluted plasma to detect PYY (total). The assay was read on a Luminex 100 analyzer. Results were analyzed against a standard curve and concentrations were determined using Milliplex Analyst 5.1 software. Values were plotted and analyzed using GraphPad Prism. Statistical analyses were conducted using multiple t-tests.

2.8 | Growth phenotyping

Male and female mice were dually housed with same sex, same genotype animals of similar weight to collect weekly food intake (standard chow or DIO) and growth data. Mouse lean and fat mass body composition was obtained by NMR (mq10 Minispec; Bruker; Billericia, MA).

2.9 | Metabolic studies

This article is protected by copyright. All rights reserved

Author Manuscript

Glucose tolerance testing was conducted as previously described [34]. Three days prior to GTT, body composition was obtained to determine lean body mass. Mice were then habituated to consecutive, daily handling sessions. On the study day, mice were fasted for 6 h from 9am- 3pm. Mice were scruffed to obtain a basal glucose read by tail nick, then injected with 1(DIO) to 2 (chow) mg/kg lean mass dose of glucose in sterile PBS. tail vein bleed at 15, 30, 45, 60, 90, and 120 min following injections Glucose readings were obtained by. Lean mass was determined by NMR body composition scan (mq10 Minispec; Bruker; Billericia, MA). Repeated sampling by tail vein bleeding was done at least 1 week apart to allow for complete recovery from blood loss. Area under the curve (AUC) was calculated by the trapezoidal rule.

2.10 | Statistical analysis and reproducibility

Sample size for growth curve studies was chosen using the power equation (α <0.05, β = 0.1, $\Delta\mu$ = 25% σ = 5), whereas sample sizes for remaining studies were estimated based on previous publications. All statistical tests were conducted using GraphPad Prism 6 software (Scientific Software; La Jolla, CA). Data are presented as mean ±standard error of the mean. All data with P<0.05 was considered statistically significant. Statistical nomenclature: * =P < 0.05; **P<0.005; ***P<0.001; ****P<0.0001. Experimental performers were generally blinded for initial studies and partially blinded for genotype identity for repeated studies. Experiments were repeated at least three times with age and litter matched animals across experimental and control groups.

3 | Results

3.1 | Global and tissue-specific deletion of *Kcnj13*

In order to analyze the potential roles of Kir7.1 in MC4R neurons *in vivo*, we developed a versatile, transgenic mouse strategy (Figure S1) using the Knockout Mouse Project (KOMP) mutant allele repository. After germ line transmission, the first generation mutant was a homozygous, global null mouse (*Kcnj13*^{KO}). As previously

This article is protected by copyright. All rights reserved

Author Manuscript

reported using a Velocigene method, we confirmed the *Kcnj13*^{KO} resulted in early (P0) postnatal lethality (Figure S2) [35]. Pathological analyses indicated retardation of lung and kidney development and failure to suckle as likely sources of lethality. We next derived a floxed line by crossing these animals with a flippase recombinase transgenic C57Bl/6NJ line. Mice expressing *Kcnj13* flanked by loxP sequences (*Kcnj13*$^{fl/fl}$) were confirmed by genotyping. Tissue specific *Kcnj13* knockout mice were then derived using the Cre-loxP method. *Kcnj13*$^{fl/fl}$ mice were crossed with mice expressing the alleles *Kcnj13*$^{fl/fl}$ and *MC4R-t2A-Cre Tg/+* (*MC4R*^{Cre}) to generate a MC4R cell specific *Kcnj13* knockout experimental animal, hereafter referred to as *Kcnj13ΔMC4R*^{Cre} (Table 1).

3.2 | Defective α-MSH-induced depolarization of MC4R PVN neurons from *Kcnj13ΔMC4R*^{Cre} mice

Kcnj13 is expressed at low levels in the sparsely distributed MC4R neurons in the CNS [32]. Thus, it is challenging to demonstrate tissue specific deletion of *Kcnj13* using mRNA expression. However, we had previously developed a functional assay of Kir7.1 in a hypothalamic slice preparation [32]. In this assay, Kir7.1 was demonstrated pharmacologically to be required for α-MSH-induced depolarization of MC4R neurons in the paraventricular nucleus of the hypothalamus. We chose to use this assay to test for Kir7.1 activity in MC4R neurons in *Kcnj13ΔMC4R*^{Cre} mice. In order to characterize the necessity of Kir7.1 for α-MSH induced depolarization of MC4R-expressing neurons within the paraventricular nucleus (PVN), electrophysiological slices were prepared from control *Kcnj13*$^{+/+}$*;MC4R*^{Cre} and *Kcnj13 ΔMC4R*^{Cre} mice, in which MC4R neurons are transgenically labeled with GFP. Whereas a 250nM bath application of α-MSH successfully depolarized PVN MC4R neurons in recordings from control mice (Figure 1A), depolarization did not occur in recordings from PVN MC4R neurons from Kcnj13ΔMC4RCre mice (Figure 1B). These data show the absence of a characterized Kir7.1 response in *Kcnj13ΔMC4R*^{Cre} mice, thereby supporting the argument that Kir7.1 is not expressed in mutant *Kcnj13ΔMC4R*^{Cre} PVN neurons, and that Kir7.1 is required for α-MSH induced depolarization in this electrophysiological slice assay. Data on the right shows representative traces from individual MC4R neurons in each genotype; bar graphs

This article is protected by copyright. All rights reserved

Author Manuscript

indicate membrane potential of MC4R neurons from each genotype, before and after α-MSH treatment.

3.3 | Defective anorexic response to melanocortin peptides in *Kcnj13ΔMC4R*^{Cre} mice

Because the absence of Kir7.1 disrupted α-MSH induced neuronal depolarization in PVN MC4R neurons in an *ex vivo* slice preparation, we hypothesized that feeding behavior in response to melanocortin agonist administration might also be adversely affected. To investigate the physiological effect of an MC4R agonist on MC4R neurons in the absence of Kir7.1 *in vivo*, we administered the potent α-MSH analogue, LY2112688 (LY), at the beginning of the dark cycle, after a 16-24 hour fast, and measured food intake. Despite the powerful drive to restore energy stores resulting from a state of nutritional deficit, LY2112688 blunted the fasting-induced refeeding response in control genotype groups, however in *Kcnj13ΔMC4RCre* male (Figure 2A) and female (Figure 2B) mice the duration of LY2112688 action was reduced. Notably, from three hours post refeeding in males and four hours post refeeding in females to twelve hours later, mice with MC4R specific deletion of Kir7.1 show a significantly reduced anorectic response to LY2112688 compared to *Kcnj13*$^{fl/fl}$ in males and *Kcnj13*$^{fl/fl}$ or *Kcnj13*$^{+/+}$*;MC4R*^{Cre} control groups in females. Additionally, at 13 and 24 hours there is no significant difference between the action of saline or LY2112688 administered to *Kcnj13ΔMC4R*^{Cre} males, while feeding in control *Kcnj13*$^{fl/fl}$ animals injected with LY2112688 remained suppressed.

This study paradigm was repeated using male mice following bilateral lentiviral *Kcnj13* shRNA knockdown, or administration of a scrambled control lentivirus in the PVN (sc shRNA). Three different lentivirus constructs designed to knockdown Kcnj13 were purchased, and tested for efficacy using HEK293 cells expressing Kcnj13 (Figure S3). A virus yielding >70% reduction in *Kcnj13* mRNA levels (Clone #99) was selected for these experiments. After 3 weeks recovery mice were acclimated to handling and injection before beginning the fast-induced refeeding study (Figure 2C). Similar to genetic deletion of Kir7.1, viral knockdown of Kir7.1 exclusively in the PVN also reduced the duration of the anorectic activity of LY2112688. LY2112688 was no longer

This article is protected by copyright. All rights reserved

Author Manuscript

effective at reducing food intake compared to saline in Kir7.1 knockdown animals from 12 hours post refeeding through 40 hours. Conversely, LY2112688 significantly reduced chow consumption in mice with intact Kir7.1 for the duration of the study. Successful targeting and delivery of *Kcnj13* shRNA or sc shRNA lentiviral vectors were confirmed by GFP expression localized to the PVN in post-mortem mice (not shown). Taken together these data show that Kir7.1 expression was required for the extended duration of anorectic response to a melanocortin peptide.

We have previously shown the role of Kir7.1 in mediating a G-protein independent MC4R response in both hypothalamic slices and in cells transfected with MC4R and Kir7.1 [32]. These electrophysiological and pharmacological experiments also demonstrated that AgRP appeared to open Kir7.1 channels in a MC4R-dependent manner [32]. To study whether Kir7.1 is necessary for AgRP-induced stimulation of food intake we delivered AgRP intracerebrventricularly (ICV) to mice in a fed state. Cannulas were implanted in the lateral ventricle of $Kcnj13^{fl/fl}Kcnj13^{+/+};MC4R^{Cre}$, and $Kcnj13\Delta MC4R^{Cre}$ male mice, and animals were allowed to recover for 5 days. Two days after a saline injection to establish baseline conditions, 1 μg of the peptide AgRP was injected ICV during the light cycle. We observe no significant difference in central AgRP induced feeding initiation or duration between genotypes (Figure S4A), suggesting Kir7.1 was not required for the orexigenic response to AgRP. Likewise, all genotypes responded to AgRP with an increase in body weight in proportion to the increase in food intake (Figure S4B). There is no significant difference in change in body weight between genotypes.

3.4 | Normal melanocortin-stimulated PYY release in $Kcnj13\Delta MC4R^{Cre}$ mice

Whereas MC4R is expressed in many brain nuclei, peripheral expression has also been mapped. Notably, MC4R is expressed in enteroendocrine L cells, and peripheral administration of α-MSH has been demonstrated to induce MC4R-dependent release of PYY and GLP1 from these cells [36]. Thus, the function of MC4R on L cells can be assessed using an assay for increased plasma PYY following peripheral administration of an MC4R agonist. We next examined the requirement for Kir7.1 in MC4R-mediated

This article is protected by copyright. All rights reserved

Author Manuscript

PYY release from L cells. The absence of Kir7.1 in MC4R cells did not interfere with the release of the satiety factor PYY into plasma (Figure 3). Thus, the role of Kir7.1 in MC4R function appeared to be important in neurons of the PVN, but not enteroendocrine L cells.

3.5 | Phenotypic characterization of *Kcnj13ΔMC4R^{Cre}* mice

Global deletion of MC4R in the mouse can produce measurable increases in adipose mass as early as 5 weeks of age [8]. To determine the effects of Kir7.1 ablation on MC4R signaling, we studied body weight, body composition, feeding behavior, and glucose tolerance in *Kcnj13 ΔMC4R^{Cre}* and control *Kcnj13$^{fl/fl}$*, *Kcnj13$^{+/+}$;MC4R^{Cre}* , and *Kcnj13$^{+/+}$;MC4R$^{+/+}$* mice. At 20 weeks of age, we did not observe differences in body weight in the four strains maintained on normal mouse chow (Figure 4A-B). Moreover, when lean and fat mass accrual are compared in young 12 week old mice and mature mice, no significant difference is detected in lean or fat mass between groups (Figure 4D-G). However, by 26 weeks of age in female and 50 weeks of age in male mice, *Kcnj13ΔMC4RCre* animals show significantly greater weight compared with all three control strains (Figure 4A, B). One-way ANOVA shows *Kcnj13ΔMC4RCre* male and female mice gained significantly more weight over the time course than the control genotypes. No significant difference was observed in daily chow consumption between groups (Figure 4C). Using indirect calorimetry, no significant difference was observed in energy expenditure among the four strains (data not shown). At 28 weeks of age, female *Kcnj13ΔMC4RCre* mice weight were observed to have significantly more absolute and %fat mass compared to control genotypes (Figure 4D,F), while lean mass was unchanged (Figure 4E). Both male and female 30 week old *Kcnj13ΔMC4RCre* animals also exhibited increased length relative to all controls (Figure 4C-D), as is observed in MC4RKO mice and humans. The % lean mass (Figure 4G) was lower in *Kcnj13ΔMC4RCre* mice due to the increase in adipose mass.

Glucose utilization was assessed by IP glucose tolerance test (GTT) in female mice at 28 weeks of age. The 2mg/kg dosage of glucose was adjusted in proportion to lean body mass. Whereas all genotypes initially responded to the bolus of glucose similarly

This article is protected by copyright. All rights reserved

Author Manuscript

(Figure 4H, I), *Kcnj13 ΔMC4RCr*e mice showed impaired glucose metabolism from 45-120 minutes (Figure 4J). Impaired glucose disposal was also observed in experiments using lean 11 week old female *Kcnj13ΔMC4RCr*e mice, relative to control $Kcnj13^{fl/fl}$ mice (data not shown).

To attempt to accentuate the physiological response to the deletion of Kir7.1 in MC4R cells, male and female animals of all four genotypes were placed on high fat diet (HFD). Mice were acclimated to single housing at 8-10 weeks old and switched from chow to HFD at 10-13 weeks of age, during which time intake and growth were monitored weekly for 3 months. A clear obesogenic effect of the Cre transgene was apparent in genotypes with or without *Kcnj13* under these conditions, perhaps due to reduction of functional MC4R resulting from the method of Cre expression, requiring cleavage of an MC4R-Cre fusion protein expressed under the control of the endogenous MC4R promoter (Figure S1). This method may result in reduced expression of MC4R protein, and/or a MC4R protein with reduced activity, due to the small t2A peptide fragment that remains at the end of the MC4R. Nonetheless, increased weight of male and female $Kcnj13\,\Delta MC4R^{Cre}$ was apparent, when compared with MC4R-Cre controls. A mixed linear effect statistical model, an alternative to ANOVA with repeated measures, was used to analyze the growth curves. This modeling tool determined that the male *Kcnj13ΔMC4RCr*e weight gain profiles (Figure 5A) are significantly greater than the *Kcnj13+/+;MC4RCre* controls. Female weight gain trended higher, and was also significantly different on HFD using student's t-tests at individual time points from 70-84 days (Figure 5C). We were unable to measure an effect of any genotype on food intake (Figure 5B, D). After consuming high fat diet for 3 months there is a significant increase in fat mass in both *Kcnj13ΔMC4RCre* and *Kcnj13+/+;MC4RCre* groups (Figure 5E-H), however we were unable to measure an effect of Kir7.1 deletion, perhaps due to the significant background effect of the Cre transgene (Figure 5E-H).

We next tested glucose utilization by IPGTT. Glucose doses at 1mg/kg were adjusted in proportion to lean mass. Despite the lack of a measurable difference in adipose mass between *Kcnj13ΔMC4RCre* and *Kcnj13+/+;MC4RCre* mice, male and female *Kcnj13ΔMC4RCre* mice have significantly reduced glucose tolerance compared with all control strains, including *Kcnj13+/+;MC4RCre* (Figure 5I-L).

This article is protected by copyright. All rights reserved

Author Manuscript

4 | Discussion

MC4R is known to signal through the Gαs-cAMP signaling pathway in cell assays and *in vivo* (29, 50). However, our data on MC4R signaling in a hypothalamic slice preparation from the mouse suggested that the MC4R depolarizes neurons in the PVN via G protein independent regulation of the inward rectifier Kir7.1 [32]. In order to assess the potential physiological role of this MC4R-Kir7.1 signaling pathway, we used Cre-loxP technology to delete Kir7.1 from MC4R-expressing cells in the mouse, and studied the consequences on MC4R signaling and on MC4R-mediated physiological responses.

Homozygous loss of Kir7.1 is known to cause degenerative eye diseases such as snowflake vitreoretinal degeneration (SVD) and Leber congenital amaurosis (LCA) [37,38] in the human, and a pigmentary defect in the *jaguar* zebrafish [39], and thus we anticipated being able to conduct our studies in the global Kir7.1 knockout mouse. Surprisingly, however, we discovered that homozygous deletion of Kir7.1 in the mouse caused perinatal lethality. Histological analysis demonstrated stunted lung and kidney development as well as reduced body mass (Figure S2), and this same finding has been reported by another laboratory [35]. It is unclear why Kir7.1 is an essential developmental gene in the mouse but not zebrafish or humans, but the observation suggests variable physiological functions of this channel in different species.

After proceeding through a breeding strategy to obtain animals with a floxed *Kcnj13* allele, we generated animals with MC4R-site specific deletion of Kir7.1. Since Kir7.1 is expressed at very low levels in the sparsely distributed MC4R neurons [32], we were not able to readily validate the absence of Kir7.1 mRNA from MC4R neurons. Recording from MC4R labeled cells in the PVN is a well-established tool for characterizing MC4R firing activity [40]. Likewise, the depolarization signature of MC4R cells via closure of Kir7.1 has been defined in the slice preparation [32]. Using this functional assay, we observed depolarization of PVN MC4R neurons from *Kcnj13+/+;MC4RCre* mice in response to α-MSH (Figure 1A). In contrast, with the deletion of Kir7.1 in MC4R PVN neurons in *Kcnj13ΔMC4R*^{Cre} mice, α-MSH induced depolarization was no longer observed (Figure 1B), supporting the hypothesis that Kir7.1

This article is protected by copyright. All rights reserved

Author Manuscript

is required for α-MSH-induced depolarization of PVN MC4R neurons in the slice preparation. We have not surveyed this requirement for Kir7.1 in other MC4R neurons depolarized by α-MSH. Furthermore, we do not know how depolarization of PVN MC4R neurons in the slice preparation correlates with the physiological sequelae of MC4R activation *in vivo*. Interestingly, while administration of MC4R agonists rapidly inhibits food intake (e.g. Figure 2), inhibition of food intake via optogenetic or chemogenetic activation of POMC neurons [41 42] has a latency of several hours. Thus, it is possible that activation of MC4R neurons in a slice preparation reflects pharmacological, but not necessarily physiological activation of the MC4R.

To study the role of Kir7.1 in mediating the pharmacological response to melanocortin agonist in vivo, we began by quantifying the feeding response on regular chow in response to an anorexigenic dose of exogenously administered α-MSH analogue, LY2112688. No significant difference is observed in baseline daily chow consumption in control vs *Kcnj13ΔMC4RCre* mice (Figure 2A). While food intake was potently inhibited by IP delivery of LY2112688 in animals with intact Kir7.1 in MC4R cells, male and female animals lacking Kir7.1 exhibited a reduced responsiveness to LY2112688 throughout the study, and also exhibited a greatly reduced duration of response. Specifically, animals lacking Kir7.1 in MC4R cells lost LY2112688 responsiveness typically by 12 hours, while control strains sustained responsiveness for 24-40 hrs (Figure 2A-C). These results suggested that the sustained activity of an administered MC4R agonist requires Kir7.1. Experiments using viral knockdown of Kir7.1 in the PVN produced very similar findings, arguing that the effect was due to the acute loss of function of Kir7.1 in PVN neurons, rather than a developmental defect.

This study parallels prior work using a Tl^+ flux assay in HEK293 cells expressing MC4R and Kir7.1 to characterize the regulation of ion flux through Kir7.1 mediated by MC4R [43]. These data suggested that the G-protein mediated cAMP response peaks rapidly after α-MSH exposure, while inhibition of Tl+ flux through Kir7.1 continued long after the cAMP response ebbed [32]. While our data clearly demonstrated pharmacological defects in response to melanocortin agonists in the absence of Kir7.1, it would also be interesting to examine the effects of chronic optogenetic stimulation of POMC neurons in

This article is protected by copyright. All rights reserved

Author Manuscript

the *Kcnj13ΔMC4R*^{Cre} mouse, given the delayed anorexigenic response observed in this assay.

AgRP engages the MC4R at high affinity, but does not couple the receptor to G proteins or stimulate arrestin recruitment [44]. Thus, when we determined that AgRP stimulates MC4R-dependent opening of Kir7.1 [32], we predicted that AgRP was a biased agonist, signaling specifically via Kir7.1. We thus anticipated that the Kcnj13ΔMC4R^{Cre} would have reduced physiologic response to the inverse agonist AgRP as well. However, a preliminary study presented here demonstrated that ICV delivery of AgRP to the hypothalamus induced similar hyperphagia and 4 days of weight gain in Kcnj13ΔMC4RCre and control mice (Figure S4). Thus, contrary to our hypothesis, AgRP may not require Kir7.1 for normal signaling. Of course, these studies were also limited by virtue of being pharmacological in nature, and additional studies will need to be conducted to determine if a compensatory signaling pathway has been activated in this knockout model, such as AgRP activation of ERK phosphorylation [45 46]. Other explanations include the possibility that a) AgRP functions exclusively as an inverse agonist and competitive antagonist of MC4R driven Gαs signaling, or b) AgRP also signals via an as yet unidentified mechanism [47 48 49].

Not only is MC4R widely expressed in the CNS, sites of peripheral expression have been detected as well, namely in the peripheral nervous system and enteroendocrine L-cells [50 51 52 36]. Using an assay for detecting MC4R-dependent L-cell release of PYY in response to exogenous administration of the α-MSH analogue LY2112688, we found that the absence of Kir7.1 in MC4R cells has no effect on PYY release (Figure 3). These data clearly showed that MC4R induces PYY release in a Kir7.1 independent manner, emphasizing the point that there are multiple modes of MC4R signaling, and that some physiological MC4R signaling events are Kir7.1 independent. Elevation of cAMP in L cells has been demonstrated to stimulate PYY release [36].

Deletion or haploinsufficiency of the MC4R results in a rapid onset of phenotypes, most prominently early onset obesity characterized by both hyperphagia, reduced energy expenditure, and hyperinsulinemia, observable by 8 weeks of age [53 8 54]. To address the physiological phenotype(s) of site-specific loss of Kir7.1 in MC4R cells we studied the weight gain profile, caloric consumption, body mass composition, linear growth and

This article is protected by copyright. All rights reserved

Author Manuscript

glucose metabolism of *Kcnj13ΔMC4R*^{Cre} mice maintained on normal mouse chow. Initially, at the 9 to 15 week time points we observed no change in body weight, body composition, or metabolism in these mice. However, as mice were measured beyond 15 weeks we observed the *Kcnj13ΔMC4R*^{Cre} mice tended to gain more weight than control genotypes, particularly in females. At a year of age we observed increased weight in *Kcnj13ΔMC4R*^{Cre} male and female mice compared to *Kcnj13*$^{fl/fl}$, *Kcnj13*$^{+/+}$*;MC4R*^{Cre}, and *Kcnj13*$^{+/+}$*;MC4R*$^{+/+}$ mice, moreover female *Kcnj13ΔMC4R*^{Cre} mice gained weight more rapidly than males. (Figure 4A, B). It was interesting to note a large effect of Kir7.1 loss on linear growth at 30 weeks of age Figure 4C-D), reminiscent of an effect seen on MC4R deletion. The late onset weight gain was clearly due to increased adipose mass (Figure 4F) and not lean mass (Figure 4G), but was not accompanied by any measurable hyperphagia (Figure 4E). The lean mass adjusted, low dose glucose tolerance test indicated deterioration of peripheral glucose metabolism in *Kcnj13ΔMC4RCre* mice, associated with significant fat accrual (Figure 4J-L). Because MC4R signaling regulates glucose homeostasis in addition to excess adipose mass animals, both of which may have contributed to defective glucose utilization shown here[7]. It is possible that hyperphagia exists, but is too small to be detected, in parallel with the very slow late onset obesity.

To potentially accelerate the effects of Kir7.1 deletion, we conducted similar experiments, placing mice on high fat diets. Notably, the expression of MC4R-t2a-Cre-recombinase alone had an obesogenic effect on high fat diet fed mice (Figure 5A, C). Given the morbid early onset obesity arising from a 50% reduction in MC4R expression in mice or humans, even a very small reduction of MC4R mRNA production, or reduced production or function of the MC4R protein resulting from, for example, inefficient cleavage of the t2a site needed for release of Cre recombinase from the MC4R-Cre fusion protein could explain the obesity seen in *Kcnj13*$^{+/+}$*;MC4R*^{Cre} mice fed high fat chow. Similarly, it is possible that the 18-22aa carboxy-terminal extension on the MC4R protein, resulting from cleavage of MC4R and Cre-recombinase, produced an MC4R with slightly reduced activity. However, these remain hypotheses, as we have no data regarding the MC4R mRNA or protein made by the MC4R-t2a-Cre-recombinase construct.

This article is protected by copyright. All rights reserved

Author Manuscript

Nonetheless, when Kir7.1 was ablated from MC4R cells, male and female mice were more sensitive to diet induced weight gain than the *Kcnj13+/+; MC4RCre controls* (Figure 5A, C). This did not appear to be due to a sustained measurable hyperphagic response (Figure 5B, D). A comparison of body mass composition by NMR reveals a significant increase in fat mass in both male and female *Kcnj13ΔMC4R*^{Cre} animals when compared to and *Kcnj13+/+ and Kcnj13fl/fl* controls, but not compared to *Kcnj13+/+;MC4RCre* (Figure 5E-H). Given the significant increase in total weight, we hypothesize that the lack of a difference in fat mass in *Kcnj13ΔMC4R*^{Cre} animals vs controls may be due to lack of sensitivity of the whole animal NMR method.

After mice had matured on high fat diet, a glucose tolerance test was conducted to test glucose utilization. A low glucose dose (1 mg/kg) adjusted to lean mass was used as mice on high fat diet already have compromised glucose homeostasis [55]. Here the Cre-driver line had no intermediate phenotype, while the *Kcnj13ΔMC4R*^{Cre} male and female mice had perturbed tolerance to glucose as confirmed by a significant increase in area under the curve (Figure 5I-L). The autonomic nervous system governs central glycemia via its two arms: ChATMc4r expressing sympathetic neurons and Phox2b^{Mc4r} expressing parasympathetic neurons [53]. Mice lacking MC4R present with hyperglycemia and hyperinsulinemia that is further exacerbated during fat accrual into maturity. While PNS outflow stimulates insulin release, SNS outflow via ChAT^{Mc4r} neurons has been demonstrated to modulate glycemic tone [17]. The deteriorating weight maintenance and glucose intolerance in *Kcnj13ΔMC4R*^{Cre} mice suggests that Kir7.1 may also augment MC4R signaling in ANS pathways regulating glucose homeostasis.

The data presented here show a measurable requirement for Kir7.1 in MC4R neurons for pharmacological responses to melanocortin agonists, but not antagonists. In particular, Kir7.1 may be required for sustained responses to pharmacotherapy with melanocortin agonists such as setmelanotide. It will be informative to determine if the delayed anorexigenic effect of optogenetic stimulation of POMC neurons requires Kir7.1. Likewise, given the apparent role of Kir7.1 in sustained anorexia, it may be informative to investigate the role of Kir7.1 in mediating the demonstrated role of MC4R signaling in disease cachexia in the mouse [56]. Similarly, other physiological responses to

This article is protected by copyright. All rights reserved

Author Manuscript

melanocortins, such as those involved in the control of glucose homeostasis, may depend on Kir7.1.

We were surprised in this study to note the very modest effect of Kir7.1 on body weight, and the divergence of the phenotype from that seen in MC4R knockout mice and patients with MC4R mutations. Indeed, all mutations leading to defective MC4R signaling, including mutations in MC4R, POMC, deletion of GαS in MC4R cells, and even overexpression of AgRP lead to a similar melanocortin obesity phenotype, characterized by early onset severe obesity, with hyperphagia increased linear growth, and increased lean mass. A very different phenotype, involving modest late onset obesity with no measurable hyperphagia, increased linear growth, and no increase in lean mass was instead observed in mice lacking Kir7.1 in MC4R cells. There are many potential explanations for these findings, including changes that compensate early on for the absence of Kir7.1. Recently, a rather dramatic example has been published illustrating the tremendous compensatory plasticity of the melanocortin circuits in response to early developmental gene knockout [57]. Deletion of leptin receptor from AgRP neurons is found to produce only a minor obesity and diabetes phenotype [58], relative to global leptin receptor deletion. In contrast, CRISP-mediated deletion of the gene in AgRP neurons in adult animals produced a morbid obesity syndrome nearly paralleling that seen in the *db/db* mouse [57]. Even more relevant to this study, leptin hyperpolarizes neurons by opening the K_{ATP} channel [59]. While global deletion of the Kir6.2 subunit of this channel had limited effect on glucose homeostasis and no obesogenic effect [60,61], CRISPR-mediated mutagenesis of Kir6.2 in AgRP neurons alone yielded a morbid obesity syndrome with diabetes [57]. Thus, it is possible that a wholly different phenotype may be seen upon deletion of Kir7.1 in the adult mouse.

Alternatively, results shown here may argue Kir7.1 plays a very specific and limited role in the physiological functioning of the MC4R. Additionally, the data shown here do not rule out the possibility that the phenotype results from a minor developmental alteration in a subset of MC4R neurons. Furthermore, we provide a direct example of a physiologically mediated MC4R pathway, PYY release, from L cells, that appears Kir7.1 independent. Interestingly, irrespective of the physiological role(s) for Kir7.1 in MC4R signaling, the work presented here shows a significant pharmacological effect of Kir7.1

This article is protected by copyright. All rights reserved

Author Manuscript

in vivo and in the slice preparation. These data may thus be important for the ongoing challenge of development of therapeutics acting at the MC4R, and further highlight the complexities of MC4R signaling that remain to be solved.

Author Manuscript

Acknowledgements

This study was supported by NIH RO1 DK070332 (RDC), NIH RO1 DK110403 (GLM), METP training grant NIH T32 DK07563 (MJL)EJ, and F30DK108476 (MJL). We thank Savannah Y. Williams and Heidi Moreno for their excellent technical assistance, Rachel Chandler and Stephanie King for assistance with figures, and Hakmook Kang for biostatistical analyses. We also thank Bradford Lowell for providing the *Mc4r-2A-Cre Tg/+* line (Jax Stock No. 030759). The ES cells, used for this research project were generated by the trans-NIH Knock-Out Mouse Project (KOMP) and obtained from the KOMP Repository (www.komp.org). NIH grants to Velocigene at Regeneron Inc (U01HG004085) and the CSD Consortium (U01HG004080) funded the generation of gene-targeted ES cells for 8500 genes in the KOMP Program and archived and distributed by the KOMP Repository at UC Davis and CHORI (U42RR024244). For more information or to obtain KOMP products go to www.komp.org or email service@komp.org.

REFERENCES

1. Vaisse C, Clement K, Guy-Grand B, Froguel P. A frameshift mutation in human MC4R is associated with a dominant form of obesity. *Nature Genetics*. 1998; **20**: 113-4.
2. Yeo GS, Farooqi IS, Aminian S, Halsall DJ, Stanhope RG, O'Rahilly S. A frameshift mutation in MC4R associated with dominantly inherited human obesity. *Nature Genetics*. 1998; **20**:111-2.

This article is protected by copyright. All rights reserved

3. Alharbi KK, Spanakis E, Tan K, Smith MJ, Aldahmesh MA, O'Dell SD, Sayer AA, Lawlor DA, Ebrahim S, Davey Smith G, O'Rahilly S, Farooqi S, Cooper C, Phillips DI, Day IN. Prevalence and functionality of paucimorphic and private MC4R mutations in a large, unselected European British population, scanned by meltMADGE. *Hum Mutat*. 2007; **28**:294-302.
4. Farooqi IS, Keogh JM, Yeo GS, Lank EJ, Cheetham T, O'Rahilly S. Clinical spectrum of obesity and mutations in the melanocortin 4 receptor gene. *The New England Journal of Medicine*. 2003; **348**:1085-95.
5. Branson R, Potoczna N, Kral JG, Lentes KU, Hoehe MR, Horber FF. Binge eating as a major phenotype of melanocortin 4 receptor gene mutations. *The New England Journal of Medicine*. 2003; **348**:1096-103.
6. Butler AA, Cone RD. Knockout models resulting in the development of obesity. *Trends Genet*. 2001; **17**:S50-4.
7. Fan W, Dinulescu DM, Butler AA, Zhou J, Marks DL, Cone RD. The central melanocortin system can directly regulate serum insulin levels. *Endocrinology*. 2000; **141**:3072-9.
8. Huszar D, Lynch CA, Fairchild-Huntress V, Dunmore JH, Fang Q, Berkemeier LR, Gu W, Kesterson RA, Boston BA, Cone RD, Smith FJ, Campfield LA, Burn P, Lee F. Targeted disruption of the melanocortin-4 receptor results in obesity in mice. *Cell*. 1997; **88**:131-41.
9. Qi L, Kraft P, Hunter DJ, Hu FB. The common obesity variant near MC4R gene is associated with higher intakes of total energy and dietary fat, weight change and diabetes risk in women. *Human Molecular Genetics*. 2008; **17**:3502-8.
10. Loos RJ, Lindgren CM, Li S, Wheeler E, Zhao JH, Prokopenko I, Inouye M, Freathy RM, Attwood AP, Beckmann JS, Berndt SI, Jacobs KB, Chanock SJ, Hayes RB, Bergmann S, Bennett AJ, Bingham SA, Bochud M, Brown M, Cauchi S, Connell JM, Cooper C, Smith GD, Day I, Dina C, De S, Dermitzakis ET, Doney AS, Elliott KS, Elliott P, Evans DM, Sadaf Farooqi I, Froguel P, Ghori J, Groves CJ, Gwilliam R, Hadley D, Hall AS, Hattersley AT, Hebebrand J, Heid IM, Lamina C, Gieger C, Illig T, Meitinger T, Wichmann HE, Herrera B, Hinney A, Hunt SE, Jarvelin MR, Johnson T, Jolley JD, Karpe F, Keniry A, Khaw KT,

This article is protected by copyright. All rights reserved

Author Manuscript

Luben RN, Mangino M, Marchini J, McArdle WL, McGinnis R, Meyre D, Munroe PB, Morris AD, Ness AR, Neville MJ, Nica AC, Ong KK, O'Rahilly S, Owen KR, Palmer CN, Papadakis K, Potter S, Pouta A, Qi L, Randall JC, Rayner NW, Ring SM, Sandhu MS, Scherag A, Sims MA, Song K, Soranzo N, Speliotes EK, Syddall HE, Teichmann SA, Timpson NJ, Tobias JH, Uda M, Vogel CI, Wallace C, Waterworth DM, Weedon MN, Willer CJ, Wraight, Yuan X, Zeggini E, Hirschhorn JN, Strachan DP, Ouwehand WH, Caulfield MJ, Samani NJ, Frayling TM, Vollenweider P, Waeber G, Mooser V, Deloukas P, McCarthy MI, Wareham NJ, Barroso I, Kraft P, Hankinson SE, Hunter DJ, Hu FB, Lyon HN, Voight BF, Ridderstrale M, Groop L, Scheet P, Sanna S, Abecasis GR, Albai G, Nagaraja R, Schlessinger D, Jackson AU, Tuomilehto J, Collins FS, Boehnke M, Mohlke KL. Common variants near MC4R are associated with fat mass, weight and risk of obesity. *Nature Genetics*. 2008; **40**:768-75.

11. Chambers JC, Elliott P, Zabaneh D, Zhang W, Li Y, Froguel P, Balding D, Scott J, Kooner JS. Common genetic variation near MC4R is associated with waist circumference and insulin resistance. *Nature Genetics*. 2008; **40**:716-8.
12. Fan W, Boston BA, Kesterson RA, Hruby VJ, Cone RD. Role of melanocortinergic neurons in feeding and the agouti obesity syndrome. *Nature*. 1997; **385**: 165-8.
13. Marks D, Cone RD. The role of the melanocortin-3 receptor in cachexia. *Ann N Y Acad Sci*. 2003; **994:**258-66.
14. Marks DL, Ling N, Cone RD. Role of the central melanocortin system in cachexia. *Cancer Res*. 2001; **61**: 1432-8.
15. Cheung WW, Kuo HJ, Markison S, Chen C, Foster AC, Marks DL, Mak RH. Peripheral administration of the melanocortin-4 receptor antagonist NBI-12i ameliorates uremia-associated cachexia in mice. *J Am Soc Nephrol*. 2007; **18**:2517-24.
16. Cheung WW, Mak RH. Melanocortin antagonism ameliorates muscle wasting and inflammation in chronic kidney disease. *Am J Physiol Renal Physiol*. 2012; **303**:F1315-24.

Author Manuscript

This article is protected by copyright. All rights reserved

17. Rossi J, Balthasar N, Olson D, Scott M, Berglund E, Lee CE, Choi MJ, Lauzon D, Lowell BB, Elmquist JK. Melanocortin-4 receptors expressed by cholinergic neurons regulate energy balance and glucose homeostasis. *Cell Metab*. 2100; **13**:195-204.
18. Zechner JF, Mirshahi UL, Satapati S, Berglund ED, Rossi J, Scott MM, Still CD, Gerhard GS, Burgess SC, Mirshahi T, Aguirre V. Weight-independent effects of roux-en-Y gastric bypass on glucose homeostasis via melanocortin-4 receptors in mice and humans. *Gastroenterology*. 2013; **144**: 580-90.
19. Itoh M, Suganami T, Nakagawa N, Tanaka M, Yamamoto Y, Kamei Y, Terai S, Sakaida I, Ogawa Y. Melanocortin 4 receptor-deficient mice as a novel mouse model of nonalcoholic steatohepatitis. *Am J Pathol*. 2011; **179**:2454-63.
20. Perez-Tilve D, Gonzalez-Matias L, Aulinger BA, Alvarez-Crespo M, Gil-Lozano M, Alvarez E, Andrade-Olivie AM, Tschop MH, D'Alessio DA, Mallo F. Exendin-4 increases blood glucose levels acutely in rats by activation of the sympathetic nervous system. *American Journal of Physiology Endocrinology and Metabolism*. 2010; **298**: E1088-96.
21. Lim BK, Huang KW, Grueter BA, Rothwell PE, Malenka RC. Anhedonia requires MC4R-mediated synaptic adaptations in nucleus accumbens. *Nature*. 2012; **487**: 183-9.
22. Xu P, Grueter BA, Britt JK, McDaniel L, Huntington PJ, Hodge R, Tran S, Mason BL, Lee C, Vong L, Lowell BB, Malenka RC, Lutter M, Pieper AA. Double deletion of melanocortin 4 receptors and SAPAP3 corrects compulsive behavior and obesity in mice. *Proceedings of the National Academy of Sciences of the United States of America*. 2013; **110**:10759-10764.
23. Cowley MA, Pronchuk N, Fan W, Dinulescu DM, Colmers WF, Cone RD. Integration of NPY, AGRP, and melanocortin signals in the hypothalamic paraventricular nucleus: evidence of a cellular basis for the adipostat. *Neuron*. 1999; **24**:155-63.
24. Kievit P, Halem H, Marks DL, Dong JZ, Glavas MM, Sinnayah P, Pranger L, Cowley MA, Grove KL, Culler MD. Chronic treatment with a melanocortin-4 receptor agonist causes weight loss, reduces insulin resistance, and improves

This article is protected by copyright. All rights reserved

Author Manuscript

cardiovascular function in diet-induced obese rhesus macaques. *Diabetes*. 2012; **62**:490-7.

25. Chen KY, Muniyappa R, Abel BS, Mullins KP, Staker P, Brychta RJ, Zhao X, Ring M, Psota TL, Cone RD, Panaro BL, Gottesdiener KM, Van der Ploeg LH, Reitman ML, Skarulis MC. RM-493, a melanocortin-4 receptor (MC4R) agonist, increases resting energy expenditure in obese individuals. *The Journal of Clinical Endocrinology and Metabolism*. 2015; **100**:1639-45.
26. Fosgerau K, Raun K, Nilsson C, Dahl K, Wulff BS. Novel alpha-MSH analog causes weight loss in obese rats and minipigs and improves insulin sensitivity. *J Endocrinol*. 2014; **220**:97-107.
27. Collet TH, Dubern B, Mokrosinski J, Connors H, Keogh JM, Mendes de Oliveira E, Henning E, Poitou-Bernert C, Oppert JM, Tounian P, Marchelli F, Alili R, Le Beyec J, Pepin D, Lacorte JM, Gottesdiener A, Bounds R, Sharma S, Folster C, Henderson B, O'Rahilly S, Stoner E, Gottesdiener K, Panaro BL, Cone RD, Clement K, Farooqi IS, Van der Ploeg LHT. Evaluation of a melanocortin-4 receptor (MC4R) agonist (Setmelanotide) in MC4R deficiency. *Molecular Metabolism*. 2017; **6**: 1321-9.
28. Clement K, Biebermann H, Farooqi IS, Van der Ploeg L, Wolters B, Poitou C, Puder L, Fiedorek F, Gottesdiener K, Kleinau G, Heyder N, Scheerer P, Blume-Peytavi U, Jahnke I, Sharma S, Mokrosinski J, Wiegand S, Muller A, Weiss K, Mai K, Spranger J, Gruters A, Blankenstein O, Krude H, Kuhnen P. MC4R agonism promotes durable weight loss in patients with leptin receptor deficiency. *Nat Med*. 2018; **24**:551-5.
29. Podyma B, Sun H, Wilson EA, Carlson B, Pritikin E, Gavrilova O, Weinstein LS, Chen M. The stimulatory G protein Gsalpha is required in melanocortin 4 receptor-expressing cells for normal energy balance, thermogenesis and glucose metabolism. *The Journal of Biological Chemistry*. 2018; **293**:10993-11005.
30. Sohn JW, Harris LE, Berglund ED, Liu T, Vong L, Lowell BB, Balthasar N, Williams KW, Elmquist JK. Melanocortin 4 receptors reciprocally regulate sympathetic and parasympathetic preganglionic neurons. *Cell*. 2013; **152**:612-9.

Author Manuscript

This article is protected by copyright. All rights reserved

31. Sohn JW, Elmquist JK, Williams KW. Neuronal circuits that regulate feeding behavior and metabolism. *Trends in Neurosciences*. 2013; **36**:504-512
32. Ghamari-Langroudi M, Digby GJ, Sebag JA, Millhauser GL, Palomino R, Matthews R, Gillyard T, Panaro BL, Tough IR, Cox HM, Denton JS, Cone RD. G-protein-independent coupling of MC4R to Kir7.1 in hypothalamic neurons. *Nature*. 2015; **520**:94-98.
33. Liu H, Kishi T, Roseberry AG, Cai X, Lee CE, Montez JM, Friedman JM, Elmquist JK. Transgenic mice expressing green fluorescent protein under the control of the melanocortin-4 receptor promoter. *The Journal of Neuroscience.* 2003; **23**:7143-54.
34. Ayala JE, Bracy DP, James FD, Burmeister MA, Wasserman DH, Drucker DJ. Glucagon-like peptide-1 receptor knockout mice are protected from high-fat diet-induced insulin resistance. *Endocrinology*. 2010; **151**:4678-87.
35. Villanueva S, Burgos J, Lopez-Cayuqueo KI, Lai KM, Valenzuela DM, Cid LP, Sepulveda FV. Cleft Palate, Moderate Lung Developmental Retardation and Early Postnatal Lethality in Mice Deficient in the Kir7.1 Inwardly Rectifying K+ Channel. *PloS one*. 2015; **10**(9): e0139284.
36. Panaro BL, Tough IR, Engelstoft MS, Matthews RT, Digby GJ, Moller CL, Svendsen B, Gribble F, Reimann F, Holst JJ, Holst B, Schwartz TW, Cox HM, Cone RD. The melanocortin-4 receptor is expressed in enteroendocrine L cells and regulates the release of peptide YY and glucagon-like peptide 1 in vivo. *Cell Metab*. 2014; **20**:1018-29.
37. Pattnaik BR, Shahi PK, Marino MJ, Liu X, York N, Brar S, Chiang J, Pillers DA, Traboulsi EI. A Novel KCNJ13 Nonsense Mutation and Loss of Kir7.1 Channel Function Causes Leber Congenital Amaurosis (LCA16). *Hum Mutat*. 2015; **36**:720-7.
38. Pattnaik BR, Tokarz S, Asuma MP, Schroeder T, Sharma A, Mitchell JC, Edwards AO, Pillers DA. Snowflake vitreoretinal degeneration (SVD) mutation R162W provides new insights into Kir7.1 ion channel structure and function. *PloS one*. 2013; **8**: e71744.

Author Manuscript

This article is protected by copyright. All rights reserved

39. Iwashita M, Watanabe M, Ishii M, Chen T, Johnson SL, Kurachi Y, Okada N, Kondo S. Pigment pattern in jaguar/obelix zebrafish is caused by a Kir7.1 mutation: implications for the regulation of melanosome movement. *PLoS genetics*. 2006; **2**:e197.
40. Ghamari-Langroudi M. Electrophysiological Analysis of Circuits Controlling Energy Homeostasis. *Molecular Neurobiology*. 2012; **45**:258-78.
41. Aponte Y, Atasoy D, Sternson SM. AGRP neurons are sufficient to orchestrate feeding behavior rapidly and without training. *Nat Neurosci*. 2011; 14:351-355.
42. Zhan C, Zhou J, Feng Q, Zhang JE, Lin S, Bao J, Wu P, Luo M. Acute and long-term suppression of feeding behavior by POMC neurons in the brainstem and hypothalamus, respectively. *The Journal of Neuroscience*. 2013; **33**:3624-32.
43. Litt MJ, Cone RD, Ghamari-Langroudi M. Characterization of MC4R Regulation of the Kir7.1 Channel Using the Tl(+) Flux Assay. *Methods Mol Biol*. 2018; **1684:**211-22.
44. Breit A, Wolff K, Kalwa H, Jarry H, Buch T, Gudermann T. The natural inverse agonist agouti-related protein induces arrestin-mediated endocytosis of melanocortin-3 and -4 receptors. *The Journal of Biological Chemistry*. 2006; **281**:37447-56.
45. Mo XL, Tao YX. Activation of MAPK by inverse agonists in six naturally occurring constitutively active mutant human melanocortin-4 receptors. *Biochimica et Biophysica Acta*. 2013; **1832**:1939-48.
46. Tao YX. Constitutive activity in melanocortin-4 receptor: biased signaling of inverse agonists. *Adv Pharmacol*. 2014; **70:**135-54.
47. Gropp E, Shanabrough M, Borok E, Xu AW, Janoschek R, Buch T, Plum L, Balthasar N, Hampel B, Waisman A, Barsh GS, Horvath TL, Bruning JC. Agouti-related peptide-expressing neurons are mandatory for feeding. *Nat Neurosci*. 2005; **8**: 289-91.
48. Luquet S, Perez FA, Hnasko TS, Palmiter RD. NPY/AgRP neurons are essential for feeding in adult mice but can be ablated in neonates. *Science*. 2005; **310**:683-5.

Author Manuscript

This article is protected by copyright. All rights reserved

49. Wu Q, Howell MP, Cowley MA, Palmiter RD. Starvation after AgRP neuron ablation is independent of melanocortin signaling. *Proceedings of the National Academy of Sciences of the United States of America*. 2008; **105**:2687-92.
50. Tao YX. The melanocortin-4 receptor: physiology, pharmacology, and pathophysiology. *Endocr Rev*. 2010; **31**:506-43.
51. Mountjoy KG, Jenny Wu CS, Dumont LM, Wild JM. Melanocortin-4 receptor messenger ribonucleic acid expression in rat cardiorespiratory, musculoskeletal, and integumentary systems. *Endocrinology*. 2003; **144**:5488-96.
52. Mountjoy KG, Mortrud MT, Low MJ, Simerly RB, Cone RD. Localization of the melanocortin-4 receptor (MC4-R) in neuroendocrine and autonomic control circuits in the brain. *Molecular Endocrinology*. 1994; **8**:1298-308.
53. Krashes MJ, Lowell BB, Garfield AS. Melanocortin-4 receptor-regulated energy homeostasis. *Nat Neurosci*. 2016; **19**:206-19.
54. Garfield AS, Li C, Madara JC, Shah BP, Webber E, Steger JS, Campbell JN, Gavrilova O, Lee CE, Olson DP, Elmquist JK, Tannous BA, Krashes MJ, Lowell BB. A neural basis for melanocortin-4 receptor-regulated appetite. *Nat Neurosci*. 2015; **18**:863-871.
55. McGuinness OP, Ayala JE, Laughlin MR, Wasserman DH. NIH experiment in centralized mouse phenotyping: the Vanderbilt experience and recommendations for evaluating glucose homeostasis in the mouse. *American Journal of Physiology Endocrinology and Metabolism*. 2009; **297**:E849-55.
56. Marks DL, Ling N, Cone RD. Role of the central melanocortin system in cachexia. *Cancer Res*. 2001; **61**(4): 1432-8.
57. Xu J, Bartolome CL, Low CS, Yi X, Chien CH, Wang P, Kong D. Genetic identification of leptin neural circuits in energy and glucose homeostases. *Nature*. 2018; **556**:505-9.
58. van de Wall E, Leshan R, Xu AW, Balthasar N, Coppari R, Liu SM, Jo YH, MacKenzie RG, Allison DB, Dun NJ, Elmquist J, Lowell BB, Barsh GS, de Luca C, Myers MG, Jr., Schwartz GJ, Chua SC, Jr. Collective and individual functions of leptin receptor modulated neurons controlling metabolism and ingestion. *Endocrinology*. 2008; **149**:1773-85.

This article is protected by copyright. All rights reserved

Author Manuscript

59. Spanswick D, Smith MA, Groppi VE, Logan SD, Ashford ML. Leptin inhibits hypothalamic neurons by activation of ATP-sensitive potassium channels. *Nature*. 1997; **390**:521-5.

60. Miki T, Nagashima K, Tashiro F, Kotake K, Yoshitomi H, Tamamoto A, Gonoi T, Iwanaga T, Miyazaki J, Seino S. Defective insulin secretion and enhanced insulin action in KATP channel-deficient mice. *Proceedings of the National Academy of Sciences of the United States of America*. 1998; **95**:10402-6.

61. Seghers V, Nakazaki M, DeMayo F, Aguilar-Bryan L, Bryan J. Sur1 knockout mice. A model for K(ATP) channel-independent regulation of insulin secretion. *The Journal of Biological Chemistry*. 2000; **275**:9270-7.

Author Manuscript

FIGURE LEGENDS

Figure 1 Defective α-MSH-induced depolarization of MC4R PVN neurons in *Kcnj13ΔMC4R^{Cre}* mice.

Slice electrophysiology of PVN MC4R-GFP positive neurons recorded in current clamp with bath application of 250nM α-MSH. (A) Recordings from *Kcnj13$^{+/+}$;MC4R^{Cre}*;MC4R-GFP mice in response to vehicle or α-MSH, showing induction of action potential differs significantly between and control and α-MSH in bath. A representative depolarizing response of a PVN MC4R neuron is seen on the right. (B) Recordings from *Kcnj13ΔMC4R^{Cre}*;MC4R-GFP mice show no significant response to α-MSH, P=0.11. A representative response of a PVN MC4R neuron is seen on the right. Bar graph represents mean +/- SEM of 15-35 cells. (***P<0.0001, paired t-test). DV_m, membrane potential in millivolts (mV).

Figure 2 Defective anorexic response to melanocortin agonist LY2112688 in *Kcnj13ΔMC4R^{Cre}* mice.

Feeding response in dark cycle after IP injection of saline or LY2112688 in male (A), or female (B) *Kcnj13ΔMC4R^{Cre}* , *Kcnj13$^{fl/fl}$*, and/or *Kcnj13$^{+/+}$;MC4R^{Cre}*, *Kcnj13$^{+/+}$;MC4R$^{+/+}$* and male (C) *Kcnj13* shRNA or sc shRNA lentiviral knockdown mice following 16-24hr

This article is protected by copyright. All rights reserved

fast. LY2112688 was administered at 10mg/kg (n = 4-9/group, *P<0.05, **P<0.005, ****P<0.0001, 2-way ANOVA with multiple comparisons test).

Figure 3 Normal melanocortin-stimulated PYY release in *Kcnj13ΔMC4R^{Cre}* mice.
Male and female C57BL/6J *Kcnj13ΔMC4R^{Cre}* and *Kcnj13$^{fl/fl}$* control mice were administered saline or saline containing 5mg/kg LY2112688 intraperitoneally. 15 minutes following treatment, blood was collected, and plasma prepared. Plasma was then assayed for peptide YY (PYY) using ELISA (Luminex). Points indicate mean PYY concentrations determined in duplicate from individual mouse serum samples, bars indicate means from multiple mice. (n=6-7/group, *P<0.05, student's t-test).

Figure 4 Late onset obesity develops in chow fed *Kcnj13ΔMC4R^{Cre}* mice.
Growth curves on chow diet of (A) male and (B) female mice interspersed across 3 age cohorts from 9 to 63 weeks. One-way ANOVA shows *Kcnj13ΔMC4RCre* male and female mice gained significantly more weight over the time course than the control genotypes. (C-D) Snout-to anus length of euthanized female (C) and male (D) *Kcnj13ΔMC4RCre* , *Kcnj13fl/fl*, *Kcnj13+/+;MC4RCre*, and *Kcnj13+/+;MC4R+/+* mice at the age of approximately 30 weeks. Each dot represents the snout-anus distance of one individual animal. (n = 6-25/group, **P<0.005, ****P<0.0001, multiple t-test with Holm-Sidak post-hoc test).(E) Daily chow consumption per mouse at mouse age indicated in weeks. One-way ANOVA test with Tukey's multiple comparisons. Absolute fat (F) and lean (G) mass and %fat (H) and %lean (I) mass body composition of 12wk, 22wk, and 28wk female mice. Multiple t-tests with Holms-Sidak multiple comparison test. (J-L) Plasma glucose concentration during intraperitoneal glucose tolerance test (IPGTT). 2g/kg glucose, normalized to % lean body mass, was administered to each animal. IPGTT was performed after six hour daytime fast in 28wk female animals. Comparison of the difference in total AUC shows (K) AUC from 0-120 is similar, whereas *Kcnj13ΔMC4R^{Cre}* mice differ significantly from control genotypes from (L) 45-120min. (J) multiple t-tests, (K-L) One-way ANOVA with multiple comparisons. (n = 6-12/group, *P<0.05, **P<0.005, ***P<0.0005, ****P< 0.0001).

This article is protected by copyright. All rights reserved

Author Manuscript

Figure 5 **Obesity and glucose intolerance in Kcnj13ΔMC4R^{Cre} mice on high fat diet.** Growth curves on high fat diet from (A) male and (C) female mice (n = 7-11/group, Mixed linear effect model of DIO male *Kcnj13*$^{+/+}$*;MC4R*^{Cre} vs. *Kcnj13*$^{fl/fl}$ P value < 1.1e-6, female P value < 2.2e-16. *Kcnj13*$^{+/+}$*;MC4RCre* vs. *Kcnj13ΔMC4R*^{Cre} male P value = 0.01, female P value = 0.8). (*P<0.05, **P<0.005 via multiple students t-test *Kcnj13*$^{+/+}$*;MC4R*^{Cre} vs. *Kcnj13ΔMC4R*^{Cre}). Daily high fat diet consumption of (B) male and (D) female mice. One-way ANOVA test. (E-H) Fat and lean mass body composition of male (E-F) and female (G-H) on chow vs HFD. Two-way ANOVA with Tukey's multiple comparison test. (I-L) Plasma glucose concentration during intraperitoneal glucose tolerance test (IPGTT) 1g/kg glucose, normalized to % lean body mass was administered to each animal. IPGTT was performed after eight hour daytime fast in mice fed HFD for five months in (I) male and (K) female animals. Comparison of the % difference in total AUC shows that *Kcnj13ΔMC4R*^{Cre} differs significantly from control genotypes in (J) males and (L) females. (n = 6-8/group, *P<0.05, **P<0.005, ***P<0.0005, one-way ANOVA with Tukey's multiple comparisons test).

Author Manuscript

This article is protected by copyright. All rights reserved

	MGI name	Common name
Global knockout	C57BL/6J-Kcnj13$^{tm1a(KOMP)Wtsi}$	Kcnj13^{KO}
Floxed allele	C57BL/6J-Kcnj13$^{tm1c(KOMP)Wtsi}$	Kcnj13$^{fl/fl}$
Cell-specific knockout	C57BL/6J-Kcnj13$^{tm1d(KOMP)Wtsi}$	Kcnj13ΔMC4R^{Cre}
Cre driver	Tg: C57BL/6J-MC4R-t2a-Cre	Kcnj13$^{+/+}$;MC4R^{Cre}

Table 1. Nomenclature of mouse strains used in this study.

Author Manuscript

This article is protected by copyright. All rights reserved

Author Manuscript

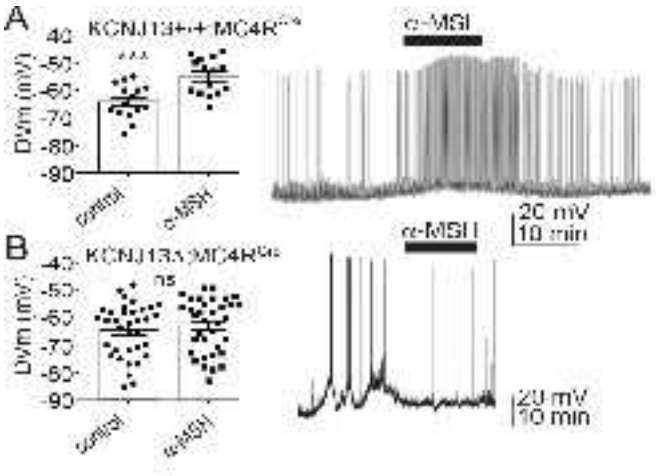

Figure 1

jne_12670_f1.tif

This article is protected by copyright. All rights reserved

Author Manuscript

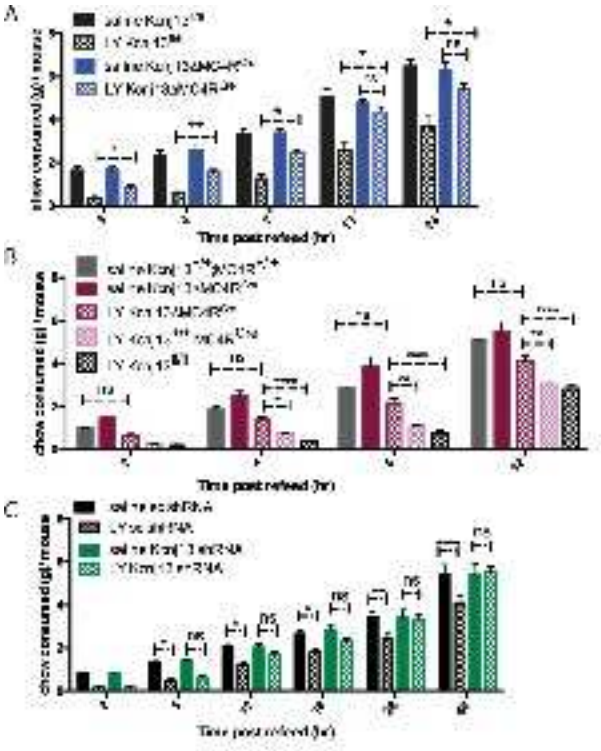

Figure 2

jne_12670_f2.tif

This article is protected by copyright. All rights reserved

Author Manuscript

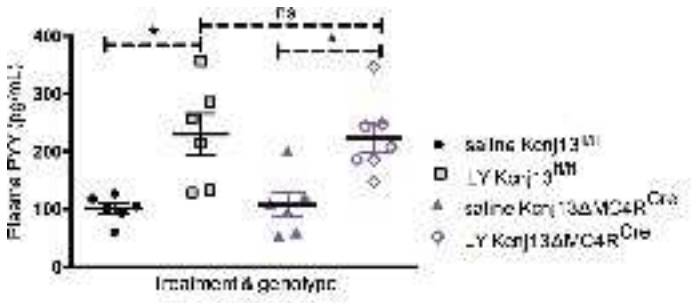

Figure 3

jne_12670_f3.tif

This article is protected by copyright. All rights reserved

Author Manuscript

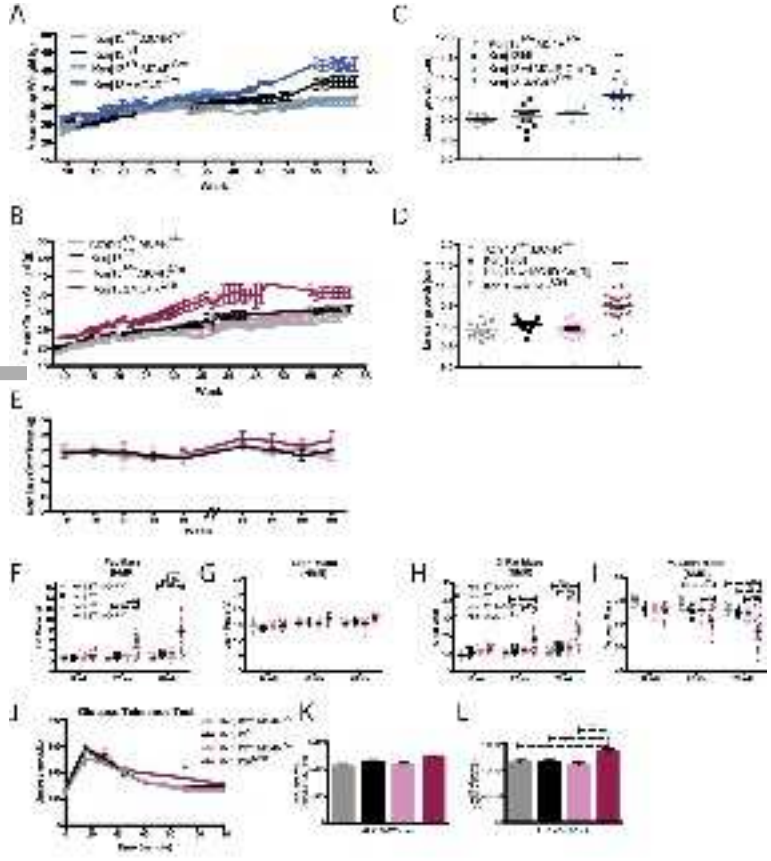

Figure 4

jne_12670_f4.tif

This article is protected by copyright. All rights reserved

Author Manuscript

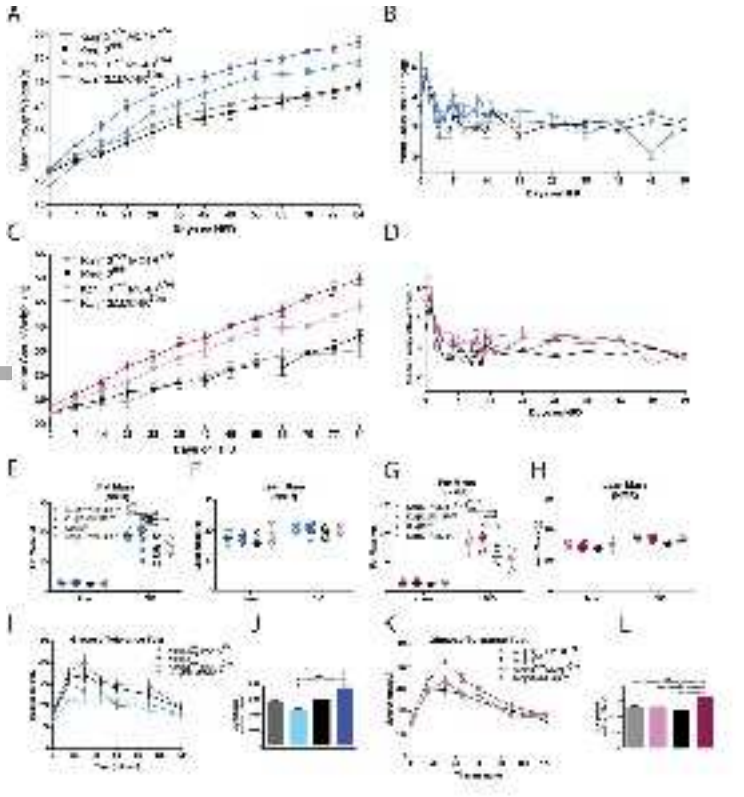

Figure 5

jne_12670_f5.tif

This article is protected by copyright. All rights reserved